Materials Characterization 135 (2018) 40–45

Contents lists available at ScienceDirect

Materials Characterization

journal homepage: www.elsevier.com/locate/matchar

Microstructural characterization of laser micro-welded Nitinol wires

Peng Dong[a,*], Hongmei Li[b], Wenxian Wang[a], Jun Zhou[c]

[a] College of Materials Science and Engineering, Taiyuan University of Technology, Taiyuan 030024, China
[b] College of Materials Science and Engineering, Jilin University, Changchun 130025, China
[c] Department of Mechanical Engineering, Pennsylvania State University Erie, Erie, PA 16563, USA

ARTICLE INFO

Keywords:
Nickel–titanium
Laser micro-welding
Transmission electron microscopy
Intermetallic

ABSTRACT

Laser micro-welding has been considered one of the most promising joining methods of manufacturing Nitinol biomedical devices. However, there is still a lack of understanding about how laser micro-welding influences the microstructure. This work attempts to reveal the phase content within various microstructural zones of laser micro-welded crossed Nitinol wires by transmission electron microscopy (TEM) with the assistance of the focused ion beam (FIB) technique. The base metal is composed of a single austenite phase (B2). The fusion zone exhibits the coexistence of austenite matrix and several intermetallics (T_2Ni, $TiNi_3$ and Ti_3Ni_4). The precipitation of R-phase was observed in HAZ with B2 matrix due to thermally induced stresses during welding.

1. Introduction

The combination of shape memory effects, superelasticity and apparent biocompatibility makes Nitinol especially suitable for the biomedical industry, wherein devices such as stents, filters, coil anchors and orthopaedic implants are manufactured [1–4]. These devices have played an important role in the progression of interventional treatments. Recently, there has been increasing clinical demand for the development of more precise and more complex devices. At present, for example, no stent can be surgically implanted into very small diameter and highly tortuous blood vessels in the brain [5–9]. However, it is difficult to fabricate such precise and/or complex stents via laser cutting due to limitations of fine tube manufacturing and economic factors. Consequently, the establishment of laser micro-welding technologies is considered one of the most promising means of fabricating Nitinol devices [8,9].

The structural characterization of phases after laser welding is of great importance, as the identification of the existing phases in a welded region is crucial to understanding the mechanical and functional behaviors of welded joints. For example, 1) amongst the different intermetallics that can form in the Ni-Ti system, Ti_2Ni [10,11] and $TiNi_3$ [12,13] are always linked to the weakening and embrittlement of Nitinol joints, owing to their inherent brittleness; 2) intermetallics precipitation has adverse effects on superelastic [14] and shape memory behaviors [15–16]; 3) modifications of chemical compositions are related to corrosion resistance [16–20] and martensitic transformation changes [14,16,21]; and 4) the grain boundary segregation of precipitates and the formation of oxides in the fusion zone (FZ) have significant effects on the properties of Nitinol joint [22,23].

Currently, the microstructural characterization of welded Nitinol joints is usually performed by X-ray diffraction (XRD). Oliveira et al. [15,24] used synchrotron X-ray radiation to probe laser welds from base material (BM) into the FZ in transmission mode. Their results revealed a significant change induced by welding: both the FZ and the heat affected zone (HAZ) showed martensite and austenite coexisting, while the base material was fully austenitic at room temperature. Several intermetallics such as Ti_2Ni [13], Ni_3Ti [12] and Ni_4Ti_3 [21] have also been found to exist in the FZ of the laser joints. However, for XRD used as a phase identification technique applied to micro-welded joints, it is difficult to ensure that the analyzed region includes only the HAZ or FZ of the specimen.

To date, very few transmission electron microscopy (TEM) analyses have been performed on micro-welded Nitinol wires. Yan et al. [17] observed the precipitation of Ti_2Ni within the FZ of austenitic base material. Chan et al. [18] showed that no precipitation occurs in the FZ after welding, which is also applied to austenitic base material, though Ni_4Ti_3 particles precipitate in the FZ after post-weld heat treatment. In particular, there are no TEM data on phases forming in the HAZ, owing to its micrometer-scale dimensions.

In this case, the preparation of TEM foil of the HAZ is impossible to accomplish using conventional method. In this work, microstructure characteristics of various zones of laser micro-welded Nitinol wires are revealed by TEM with the assistance of the focused ion beam (FIB) technique.

* Corresponding author at: College of Materials Science and Engineering, Taiyuan University of Technology, No. 79 at Yingze Western Street, Taiyuan 030024, China.
E-mail address: dongpeng@tyut.edu.cn (P. Dong).

https://doi.org/10.1016/j.matchar.2017.11.022
Received 28 August 2017; Received in revised form 9 November 2017; Accepted 9 November 2017
Available online 10 November 2017
1044-5803/

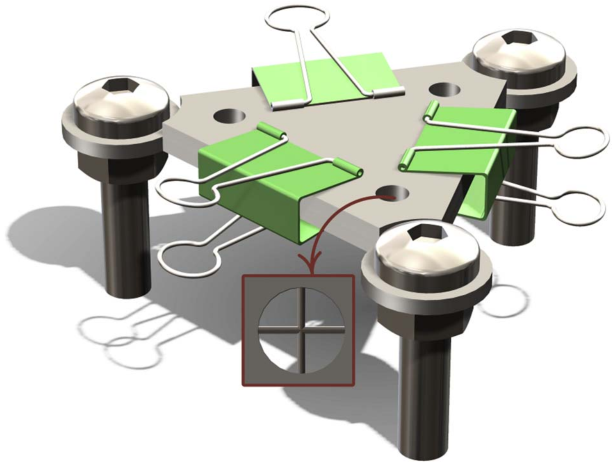

Fig. 1. Three-dimensional (3D) schematic of laser micro-welding fixture.

Table 1
Laser welding parameters used in this work.

Power/W	Pulse time/ms	Laser frequency/ Hz	Defocusing/mm	Ar shielding/ $L\cdot min^{-1}$
300	0.2	1	0	5

2. Experimental Details

The materials used were commercial superelastic Nitinol (Ti–55.8 wt% Ni) wires with a diameter of 254 μm (Confluent Medical Technologies, Inc.). Prior to welding, Nitinol wires were treated using pickling ($HF:HNO_3:H_2O$ = 1:4:5) for 20 s to remove surface oxides and contaminations followed by ultrasonic cleaning in acetone for 5 min. Next, the wires were rinsed several times with deionized water and dried with airflow.

Fig. 1 shows the 3D image of the employed welding fixture, inspiring from the published work conducted by Tam et al. [11]. The wires at 90 degrees to one another were positioned in the holes. A downward force was applied through binder clips to ensure the intimate contact and to position the wires on a single plane after welding. Wire-to-wire crossed joints were performed using pulsed Nd: YAG laser (W100B, Han's Laser). The beam was focused with the spot size of 150 μm and centered at the intercept of the crossed wires using a microscope. The laser welding parameters (shown in Table 1) were determined from our previous optimization study.

The morphology of the Nitinol wires after laser micro-welding was observed by a scanning electron microscopy (SEM; TESCAN MIRA3 LM). The microstructure of Nitinol joints was examined using a high-resolution transmission electron microscopy (HRTEM; JEOL 2100F) at an acceleration voltage of 200 kV. The TEM foil samples were prepared using an SEM/FIB crossbeam workstation (TESCAN LYRA3) from BM, HAZ and FZ of the joint.

3. Results and Discussion

Fig. 2 shows the typical morphology of a Nitinol crossed joint. The figure shows that a smooth surface without welding defects was achieved using laser micro-welding. Such a smooth surface is essential for medical implants to minimize damage to organs and tissues during implantation and operation [25]. In addition, the wires were placed onto a single plane after welding, which is beneficial for stent manufacturing. It is necessary to note that some welding defects such as lack of bonding and undercutting may occur if inappropriate welding parameters are chosen [11].

Overall SEM observations of the horizontal section of the joint are shown in Fig. 3a. The BM includes fine grains with indiscernible grain boundaries (Fig. 3b), produced during the cold drawing of Nitinol wires. Fig. 3c shows the microstructure of the FZ center, which exhibited columnar dendrites and a small number of equiaxed grains. In the HAZ (Fig. 3d), fine equiaxed grains were observed. Fig. 3e shows a mosaic SEM image illustrating that the width of HAZ is roughly 100–130 μm. Thus, FIB technique must be applied for the TEM analysis of the HAZ.

From welding metallurgy [26], the grain structure close to the fusion boundary was attributed to epitaxial growth, and the coarse columnar dendrites were generated as a result of competitive growth. In the HAZ, temperature increases supported recrystallization phenomena in cold-drawn base metal even though such processes occurred for a short period of time. As a result, the refined equiaxed grain structure was observed.

Fig. 4 shows a TEM micrograph and the corresponding selected area diffraction pattern (SADP) of the BM. Grains in the BM are preferentially oriented in a specific direction. The elongated grains are longer than 1.5 μm and approximately 40 nm wide, as shown in Fig. 4a. Consequently, it is clear that grain boundaries are undistinguishable through SEM. Furthermore, the SADP (Fig. 4b) reveals that the BM is composed of a single B2 phase.

TEM foil of the HAZ was prepared close to the fusion boundary using an FIB system and the lift-out technique [27]. The etching location is shown in Fig. 5a. The foil was finally thinned to a uniform thickness of ~50 nm (Fig. 5b). Fig. 5c shows a high magnification TEM micrograph taken from the HAZ. It is clear that several dislocations were observed with dark contrast emerging from extremely fine particles. Furthermore, Fig. 5d and e show the corresponding SADP for the $[-1\ 1\ 1]_{B2}$ and $[0\ -1\ 1]_{B2}$ zone axis, respectively. These patterns are indexed according to the B2 phase with characteristic one-third reflections, confirming features of the R-phase identity based on previous studies [28–29].

Prepared TEM foil of the FZ was positioned at the center, as shown in Fig. 6a. The foil was finally thinned to a uniform thickness of ~40 nm (Fig. 6b). Fig. 6c shows a high magnification TEM micrograph taken from the FZ, from which many nanoscale particles can be observed in the form of networks. These second-phase particles exhibited

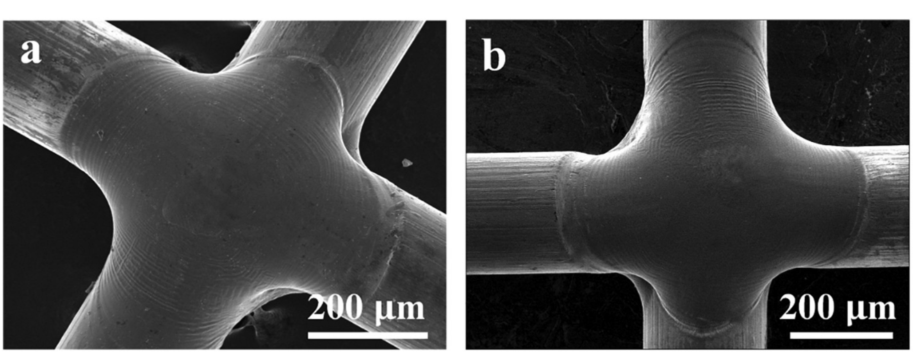

Fig. 2. FESEM observation of the crossed joint for the (a) front and (b) back surfaces.